

## Accepted Manuscript

Single and competitive sorption properties and mechanism of functionalized biochar for removing sulfonamide antibiotics from water

Mohammad Boshir Ahmed, John L. Zhou, Huu Hao Ngo, Wenshan Guo, Md Abu Hasan Johir, Kireesan Sornalingam

PII: S1385-8947(16)31668-0  
DOI: <http://dx.doi.org/10.1016/j.cej.2016.11.106>  
Reference: CEJ 16107

To appear in: *Chemical Engineering Journal*

Received Date: 15 September 2016  
Revised Date: 15 November 2016  
Accepted Date: 15 November 2016

Please cite this article as: M.B. Ahmed, J.L. Zhou, H.H. Ngo, W. Guo, M.A. Hasan Johir, K. Sornalingam, Single and competitive sorption properties and mechanism of functionalized biochar for removing sulfonamide antibiotics from water, *Chemical Engineering Journal* (2016), doi: <http://dx.doi.org/10.1016/j.cej.2016.11.106>

This is a PDF file of an unedited manuscript that has been accepted for publication. As a service to our customers we are providing this early version of the manuscript. The manuscript will undergo copyediting, typesetting, and review of the resulting proof before it is published in its final form. Please note that during the production process errors may be discovered which could affect the content, and all legal disclaimers that apply to the journal pertain.



**Single and competitive sorption properties and mechanism of  
functionalized biochar for removing sulfonamide antibiotics from  
water**

Mohammad Boshir Ahmed, John L Zhou\*, Huu Hao Ngo, Wenshan Guo, Md Abu Hasan

Johir, Kireesan Sornalingam

School of Civil and Environmental Engineering, University of Technology Sydney, 15

Broadway, NSW 2007, Australia

**Corresponding author:**

Prof John L Zhou

School of Civil and Environmental Engineering

University of Technology Sydney

15 Broadway, NSW 2007

Australia

Email: junliang.zhou@uts.edu.au

**Abstract**

Single and competitive sorption of ionisable sulphonamides sulfamethazine, sulfamethoxazole and sulfathiazole on functionalized biochar was highly pH dependent. The equilibrium data were well represented by both Langmuir and Freundlich models for single solutes, and by the Langmuir model for competitive solutes. Sorption capacity and distribution coefficient values decreased as sulfathiazole > sulfamethoxazole > sulfamethazine. The sorption capacity of each antibiotic in competitive mode is about three times lower than in single solute sorption. The kinetics data were best described by the pseudo second-order (PSO) model for single solutes, and by PSO and intra-particle diffusion models for competitive solutes. Adsorption mechanism was governed by pore filling through diffusion process. The findings from pH shift, FTIR spectra and Raman band shift showed that sorption of neutral sulfonamide species occurred mainly due to strong H-bonds followed by  $\pi^+$ - $\pi$  electron-donor-acceptor (EDA), and by Lewis acid-base interaction. Moreover, EDA was the main mechanism for the sorption of positive sulfonamides species. The sorption of negative species was mainly regulated by proton exchange with water forming negative charge assisted H-bond (CAHB), followed by the neutralization of -OH groups by  $H^+$  released from functionalized biochar surface; in addition  $\pi$ - $\pi$  electron-acceptor-acceptor (EAA) interaction played an important role.

**Keywords:** Sulfonamide antibiotics; Competitive sorption; Biochar; Functional groups:  $\pi$ - $\pi$  electron

## 1. Introduction

Antibiotics can selectively act on bacteria and pathogens without affecting human cells and tissues [1-3]. Concerning the different classes of antibiotics, sulfonamide antibiotics such as sulfamethazine (SMT), sulfamethoxazole (SMX) and sulfathiazole (STZ) are commonly used in human therapy as well as veterinary medicine because they are endowed with broad activity spectrum against Gram bacteria to prevent and control infectious diseases [4, 5]. However, a large fraction of sulfonamides remains un-metabolised through the digestive system and is released continually to soil and water due to their high water solubility [2, 6]. They can potentially damage aquatic organisms and impact on human health through the food chain [7]. Therefore the adverse impact of such compounds has received extensive attention.

Biochar has received increasing recognition as an important soil component, in carbon sequestrations and water remediation [8-13]. Owing to its high hydrophobicity and aromaticity, biochar is an excellent sorbent for hydrophobic organic contaminants e.g. aromatics [13, 14]. Biochar properties including surface functionality can be further improved through different modification technologies [15]. Studies on the adsorption of ionic organic compounds to biochar and functionalized biochar are limited compared to non-ionic hydrophobic organic contaminants [16-18]. Nonetheless, from the few studies that have used engineered carbon nanomaterials and biochars as adsorbents [17-19], it can be expected that biochar can significantly affect or even dominate the sorption of ionic organic contaminants such as sulfonamides in the environment. For example, it was observed that, under environmentally relevant conditions, distribution coefficient ( $K_d$ ) values of two sulfonamides (SMX and sulfapyridine) to multi-walled carbon nanotubes and crop residue-derived biochar can be in the order of  $10^4$  L kg<sup>-1</sup>. These are several orders of magnitude higher than the reported  $K_d$  values to soils and clay minerals [18, 19]. Adsorption of sulfonamides to biochar is expected to be heavily influenced by solution conditions and antibiotic speciation e.g. neutral, cationic or anionic forms under different pH conditions (**Figure 1**). Different species

can interact with biochar through different mechanisms [16, 17] such as  $\pi$ - $\pi$  EDA interaction, nucleophilic addition, electrostatic attraction, pore filling, partitioning into un-carbonized fraction and formation of CAHB with surface oxygen groups. This is particularly the case under alkaline conditions with multiple surface groups of sulphonamides, and with certain type of biomass materials and biochar preparatory conditions [3, 16, 20, 21].

To date, the majority of adsorption studies of different antibiotic residues have been conducted using single solutes, and studies are scarce on the competitive nature and mechanisms of antibiotic mixtures using different adsorbents. These include, for example, natural clay, activated carbon, ion exchange resins, graphene, carbon nano-tubes and biochar. This study therefore aims to bridge this gap in our knowledge so that the mechanism of single and competitive nature of three widely used sulfonamides antibiotics (sulfamethazine, sulfamethoxazole and sulfathiazole) using functionalized biochar is better understood. Their physicochemical properties are shown in the Supporting Information (**Table A1**). Laboratory experiments were conducted to elucidate and compare the single and comparative interactions of sulfonamides onto functionalized biochar. Experimental data were fitted to different isotherm models and the adsorption affinities were compared. The governing adsorption mechanisms were analysed. The effects of pH and temperature on the adsorption were examined to verify the proposed sorption mechanisms and adsorption properties. The research findings will contribute to improved understanding of the adsorption behaviour and mechanism of antibiotics mixture.

## **2. Experimental section**

### *2.1. Chemicals and reagents*

The antibiotic standards (purity > 99%) of SMT, SMX and STZ, HPLC-grade organic solvents such as methanol, acetonitrile and acetone, and analytical-grade aluminium chloride, potassium chloride and formic acid were purchased from Sigma-Aldrich, Australia.

## 2.2. Preparation of biochar and functionalized biochar

Biomass was selected for the preparation of biochar as reported in Ahmed et al. [14] (**Appendix A**). Briefly, 50 g of bamboo biomass material was cut into 0.6-2 mm size particles and placed into a fixed bed reactor. Biomass material was gradually pyrolyzed at 380 °C in a reactor inside the furnace at an average heating rate of 10-11.4 °C min<sup>-1</sup> under continuous nitrogen supply at 2.5 psi for 2 h. When the temperature reached at 380 °C, nitrogen pressure was increased to 10 psi and maintained for 20 min. The reactor was cooled at room temperature and biochar was grinded and finally washed and dried. The prepared biochar coded as BBC380.

Functionalization of BBC380 was carried out by soaking 15.3 g of BBC380 in 30 mL of 50% ortho-phosphoric acid (H<sub>3</sub>PO<sub>4</sub>) for 3 h at 50 °C. H<sub>3</sub>PO<sub>4</sub> was selected based on previous studies [15, 22]. The mixture was then heated at 600 °C for 2 h with the same heating rate as used before under continuous nitrogen supply at 2.5 psi, cooled at room temperature, and washed with distilled water 4 times while adjusting pH to 7, followed by drying overnight at 120 °C, to obtain the functionalized biochar (M1bBBC600). Average functionalized biochar particles size ranged from 75-1000 µm.

## 2.3. Characterizations of biomass, biochar and functionalized biochar

The physicochemical characteristics of raw biomass, biochar and functionalized biochar were extensively examined using Fourier transform infrared spectroscopy (FTIR), BET, Raman spectroscopy, thermo gravimetric analysis (TGA) and others (**Appendix A, Tables A2 and A3, Figure A1**). The produced samples were examined by using energy dispersive spectrometer (EDS) to determine the elemental composition of biochar and functionalized biochar (Zeiss Evo-SEM). EDS was measured on different parts of the biochars and average results are reported in Table A2. Structural analysis was conducted using FTIR (Miracle-10 from Shimadzu). The spectra were obtained at 4 cm<sup>-1</sup> resolution by measuring the absorbance

from 400 to 4000  $\text{cm}^{-1}$  using a combined 40 scans. Raman shifts measurement was carried out using Renishaw in via Raman spectrometer (Gloucestershire, UK) equipped with a 17 mW Renishaw Helium-Neon Laser 633 nm and CCD array detector. Thermo-gravimetric analysis and differential scanning calorimetry (TGA-DSC) tests were done using SDT Q600. The specific surface area and porosity distributions were calculated using Brunauer-Emmett-Teller (BET) nitrogen adsorption-desorption isotherms and the Barrett-Joyner-Halenda (BJH) method, respectively, by utilizing a Micromeritics 3-Flex<sup>TM</sup> surface characterization analyzer at 77 K. Zeta potential values were measured using 50 mg of functionalized biochar in 100 mL of 1-mM KCl solution at different pH. Samples were pre-equilibrated for 48 h. Zeta potential values were determined using a Nano-ZS Zeta-seizer (Malvern, Model: ZEN3600). Zeta potential was measured three times at each pH (50 scans each time) and the average and standard deviation was calculated.

#### *2.4. Sorption experiments using functionalized biochar*

Stock solutions of SMX, SMT and STZ were prepared with DI water in 1% methanol (insignificant co-solvent effect) without adjusting the pH. The studies on pH effect were conducted at different pH values starting from 1.5 to 10 for 24 h at room temperature to determine sorption equilibrium time. The solution pH was adjusted using 0.1 M HCl and 0.1 M NaOH solution before adding functionalized biochar. Batch single and competitive experiments were carried out at different temperatures ( $21\pm 0.5$ ,  $25\pm 0.5$  and  $30\pm 0.5$  °C) by mixing and shaking 100  $\text{mg L}^{-1}$  of functionalized biochar in 100 ml solution on an orbital shaker at 120 rpm for 40 h at a pH of 3.25, 4.50, 3.50 and 3.50, respectively, for SMX, SMT, STZ and mixtures of three antibiotics. The control experiments without adsorbents were also executed. The kinetics studies for single and competitive antibiotics were done using the same pH and adsorbent dosage as carried out in isotherm studies for 24 h. After equilibrium, final

solution pH was measured and the supernatant concentration was measured with HPLC with aliquots from each reactor being taken and filtered through a 0.20  $\mu\text{m}$  PTFE filter.

### 2.5. Analytical method

The concentrations of antibiotics were measured by HPLC (Jasco) equipped with an auto-sampler and UV detector at 285 nm, by 20  $\mu\text{L}$  injection. A reverse phase Zorbax Bonus RP  $\text{C}_{18}$  column (5.0  $\mu\text{m}$ , 2.1  $\times$  1.50 mm, Agilent Technologies) was used for the separation. Mobile phase A was composed of acetonitrile and formic acid (99.9: 0.1) while mobile phase B was composed of Milli-Q water and formic acid (99.9: 0.1). The elution used 40% of A and 60% of B at a flow rate of 0.4  $\text{mL min}^{-1}$ , which was changed to 0.2  $\text{mL min}^{-1}$  at 0.1 min. The method was run over 8 min.

### 2.6. Distribution coefficient, kinetics and isotherm equations

The adsorption data obtained in the experiments were fitted to two different isotherm models namely Langmuir and Freundlich isotherm models and three kinetic equations. The apparent sorption distribution coefficient ( $K_d$ ,  $\text{L kg}^{-1}$ ) is defined by the ratio of adsorbate concentration on sorbent ( $Q_e$ ,  $\text{mg kg}^{-1}$ ) to the adsorbate concentration in solution ( $C_e$ ,  $\text{mg L}^{-1}$ ):

$$K_d = \frac{Q_e}{C_e} = \left( \frac{C_0 - C_e}{C_e} \right) \frac{V}{M} \quad (1)$$

where  $C_0$  is the initial adsorbate concentration ( $\text{mg L}^{-1}$ ),  $V$  is the solution volume (L), and  $M$  is the sorbent mass (kg).

The kinetic equations such as pseudo first order (PFO), pseudo second order model (PSO) and intra-particle diffusion model (IDM) can be represented as follows:

$$\text{PFO: } Q_t = Q_e(1 - e^{-K_1 t}) \quad (2)$$

$$\text{PSO: } Q_t = \frac{K_2 Q_e^2 t}{1 + K_2 Q_e t} \quad (3)$$

$$\text{IDM: } Q_t = K_i t^{\frac{1}{2}} + C \quad (4)$$

where  $K_i$  is the apparent diffusion rate constant ( $\text{mg g}^{-1} \text{min}^{-1/2}$ );  $K_1$  ( $\text{min}^{-1}$ ) and  $K_2$  ( $\text{g mg}^{-1} \text{min}^{-1}$ ) are PFO and PSO kinetic rate constant, respectively;  $C$  is a constant ( $\text{mg g}^{-1}$ ) that provides the thickness of the boundary layer. These parameters were estimated by nonlinear regression weighted by the dependent variables.

The Langmuir and Freundlich isotherm models are shown below:

$$\text{Freundlich model: } Q_e = K_F C_e^{1/n} \quad (5)$$

$$\text{Langmuir model: } Q_e = \frac{Q_{\max} K_L C_e}{1 + K_L C_e} \quad (6)$$

where  $Q_{\max}$  is the maximum adsorption capacity ( $\text{mg g}^{-1}$ ),  $n$  is a dimensionless number related to surface heterogeneity,  $K_F$  is the Freundlich affinity coefficient ( $\text{mg}^{1-n} \text{L}^n \text{g}^{-1}$ ) and  $K_L$  is the Langmuir fitting parameter ( $\text{L mg}^{-1}$ ).

### 3. Results and discussions

#### 3.1. Influences of pH on distribution coefficient

Sulfonamides sorption on carbonaceous materials revealed pronounced pH dependence. The effect of pH on the sorption coefficients is shown in **Figure 2a**. Clearly, sulfonamides sorption was greatly governed by the electrostatic interactions between antibiotics and functionalized biochar surface. The distribution coefficient ( $K_d$ ) values (**equation 1**) for the sorption of sulfonamides reached their first maxima at pH 3.50 for STZ, at pH 3.25 for SMX and at pH 4.5 for SMT. A further increase of pH up to 5 (for SMX and STZ) and up to 7 (for SMT) resulted in a decrease in  $K_d$  values. Maximum sorption was due to the adsorption of neutral species of sulfonamides. Selected sulfonamides behaved as positive species at solution pH < 2.5 for SMT and STZ and pH < 1.6 for SMX (**Figure A2**). Biochar surface also became positive because the surface zeta-potential was also positive below pH 2.5. Hence less adsorption is expected due to electrostatic repulsion of positively charged biochar surface and sulfonamide antibiotics. The adsorption of antibiotics at pH < 2.5 may be dominated by the interaction between the protonated aniline ring of sulfonamide antibiotics and the  $\pi$ -electron

rich functionalized biochar surface [16, 17]. The second sharp increase in  $K_d$  values for each single solute was observed from pH 5 to 6, 5 to 6.3, and 7 to 8, for SMX, STZ and SMT respectively; which coincided with the intersections of neutral and negative species of the three compounds. This was followed by a decreasing pattern up to pH 10. These trends may be due to the shifting of pH to neutral species region of sulfonamides as a result of proton release from functionalized biochar surface. The pH test showed that final solution pH became significantly lower and shift toward neutral region if the initial solution pH was maintained at above 7. A further increase of pH up to 10, the sorption of  $\text{SMX}^-$ ,  $\text{STZ}^-$  and  $\text{SMT}^-$  species declined due to negative surface zeta-potential value and the negative surface electrostatic repulsion. However, the negatively charged biochar surface was still able to sorb to negative species from solutions through the formation of CAHB [16, 23].

### 3.2. Sorption kinetics for single and competitive solutes

The kinetics of sulfonamide antibiotics sorption by functionalized biochar at different times were fitted to pseudo-first-order (PFO), pseudo-second-order (PSO) and intra-particle diffusion model (IDM) as presented in equations 2-4. Based on the correlation coefficient ( $R^2$ ) and  $Q_{e,cal}$  values, the kinetics of sorption for all single solutes closely followed the PSO chemisorption kinetic model rather than PFO and IDM [24] (**Figures 2b and A3**). Moreover, IDM may not be the best model to describe the rate controlling mechanism of single solutes as  $R^2$  value was significantly lower than PSO plot (Table A4). The values of PSO rate constant  $K_2$  and IDM rate constant  $K_i$  decreased as  $\text{SMX} > \text{SMT} > \text{STZ}$  and  $\text{STZ} > \text{SMX} > \text{SMT}$ , respectively, for single solutes.

IDM showed higher  $R^2$  values than the PSO model (**Table A4**), suggesting the competitive sorption kinetics of sulfonamide antibiotics on functionalized biochar were controlled by a diffusion-dominated mechanism, which is consistent with a previous study [25], and can be explained by the PSO. Other processes such as the boundary layer diffusion

or external mass transfer may also regulate the sorption process.  $Q_{e,cal}$  values were higher for PSO than those of PFO. The  $K_i$  values followed the order  $STZ > SMX > SMT$  for competitive solutes. Maximum sorption capacities for PSO followed the trend of  $STZ > SMX > SMT$ .

### 3.3. Sorption affinity and temperatures effect

Single and competitive sorption isotherm plots for the Langmuir and Freundlich isotherm models (equations 5 and 6) are presented in **Figures 3, A4 and A5**. The model parameters are summarized in **Tables A5 and A6**. The sorption data for single solute STZ and SMX were fitted by both the Freundlich and Langmuir isotherm models. However, the sorption data for SMT was fitted slightly better by the Freundlich model with higher  $R^2$  values. Maximum Langmuir adsorption capacity ( $Q_{max}$ ) values were 237.71, 65.74 and 88.10  $mg\ g^{-1}$ , respectively, for STZ, SMT and SMX at 25 °C. Adsorption capacity was increased significantly for STZ (85%) and SMT (55%) and slightly for SMX (5%) when the temperature rose from 21 to 25 °C. A further increase in temperature from 25 to 30 °C decreased the adsorption capacity while the distribution coefficient indicated that adsorption was unfavorable through monolayer covering. This is likely due to the complex relation between chemical activation energy and exothermic reaction nature of adsorption. Specifically there is a need for temperature increase to overcome activation energy (from 21-25 °C), but further increase above 25 °C caused a decrease in adsorption which releases heat. Sorption affinity could be ranked as follows:  $STZ > SMX > SMT$ . Conversely, the maximum Freundlich constant  $K_F$  values with higher  $R^2$  values were found to be 22.12, 21.33 and 21.86  $mg^{1-n} L^n g^{-1}$  for STZ, SMT and SMX respectively, at 25 °C. These results could happen due to specific surface area, microspore volume, and introduction of additional sites onto functionalized biochar [26, 27]. The  $K_d$  values for single solute ranged between  $2.56 \times 10^3$  and  $8.57 \times 10^4$ ,  $1.0 \times 10^3$  and  $5.77 \times 10^4$ , and  $1.8 \times 10^3$  and  $6.4 \times 10^4$   $L\ kg^{-1}$ , for STZ, SMT and SMX respectively (**Figure 4b**). The observed  $K_d$  values,  $Q_{max}$  and  $K_F$  values for single solute

of STZ, SMX and SMT were higher than reported in other studies using different adsorbents e.g. carbon nanotubes (CNTs) supported nano-composite and graphene-oxide based adsorbents and carbonaceous nano-composites [13, 24, 26-33]. For example, biochar prepared at 700 °C from Burcucumber plants was found to show the maximum sorption capacities of 20.56 and 37.73 mg g<sup>-1</sup>, respectively for biochar (700 °C) and steam modified biochar [27]. In addition, biochars prepared from *Salvia miltiorrhiza* Bunge biomass at 600 and 800 °C showed the maximum K<sub>F</sub> values of 0.0155 and 0.0257 mg<sup>1-n</sup> L<sup>n</sup> g<sup>-1</sup>, respectively for the removal of sulfamethoxazole [13].

Competitive removal of sulfonamide antibiotics was found to be better fitted to the Langmuir isotherm model with higher R<sup>2</sup> values and the maximum sorption capacities were obtained at 25 °C. The sorption affinity was the same as that for single solutes. Competitive Q<sub>max</sub> values were found to be 40.11, 34.01 and 25.11 mg g<sup>-1</sup>, for STZ, SMX and SMT respectively, at 25 °C. The maximum K<sub>F</sub> values were 12.46, 10.46 and 11.06 mg<sup>1-n</sup> L<sup>n</sup> g<sup>-1</sup>, respectively, for STZ, SMT and SMX at 21 °C. The K<sub>d</sub> values for competitive solutes ranged from 2.0×10<sup>3</sup> and 2.5×10<sup>4</sup>, 1.2×10<sup>3</sup> and 2.21×10<sup>4</sup>, and 1.6×10<sup>3</sup> and 2.37×10<sup>4</sup> L kg<sup>-1</sup>, for STZ, SMT and SMX respectively (Figure 4a). Further increases in temperature from 25 to 30 °C led to a decline in sorption affinity and K<sub>d</sub> indicated that adsorption affinity was not strong enough to support homogeneous covering of the surface. Kinetics and isotherms data indicated that competitive sorption of sulfonamide solutes was better fitted by the Langmuir model.

Total sorption capacities of the competitive solutes were calculated (**equations A3 and A5**) by adding individual contributions to the overall sorption for both Langmuir and Freundlich models. When comparing the single solute sorption capacities, each competitive solute was found to have nearly 2-fold less adsorption capacity for overall individual sorption capacities. Overall sorption capacities of competitive solutes are almost analogous to near about the maximum sorption capacities of individual solutes sorption capacities. Hence the

total sorption capacities of competitive solutes onto adsorbent surface were maintained at a similar level to single solute sorption. The results indicated that sorption on biochar was of monolayer coverage in nature.

#### 3.4. Diffusion of sorbate molecules

Based on our kinetics study, the competitive adsorption mechanism for STZ, SMT and SMX can partly be postulated firstly as a monolayer process involving sorbate molecules transportation and diffusion. It is a process controlled by a combination of mass transfer steps relating to external, surface microlayer, pore diffusion and adsorption on biochar surface, thus supporting IDM mechanism (**Figure 5**). Secondly, both single and competitive solutes followed the PSO kinetic model with adsorption through chemisorption with the surface functional groups being indicated. Based on the isotherm study, this can be attributed, to the adsorption of STZ and SMX following the monolayer through diffusion and chemisorption reactions with surface functional groups in biochar. Adsorption of SMT followed the Freundlich isotherm which was related to the chemisorption mechanism. In comparison to biochar, the functionalized biochar had its surface area increased by 2.3 folds while its pore diameter reduced to half. In addition, its Langmuir surface area was increased by 68 times compared to that of biochar. Moreover, BJH and Dollimore Heal (D-H) adsorption cumulative surface area of functionalized biochar was increased by 6 folds compared to biochar. However, BJH and D-H pore diameters of biochar were 113 and 154 Å which decreased to 84 and 78 Å after functionalization (**Table A3**). Thus, higher adsorption affinities of functionalized biochar may be partly due to the increase in surface area and reduction in pore diameter, accompanied by active adsorption sites facilitating the adsorption of neutral sulfonamide molecules. This occurred through diffusion rather than sorption chemisorption. The IDM rate constant values  $K_i$  indicated that the diffusion of the

sulfonamide molecules (both single and competitive solutes) toward biochar surface followed the trend of STZ > SMX > SMT.

### 3.5. Lewis acid-base interaction

Based on the structural composition of the sulfonamides, they consist of sulfonamide group (para position at benzene ring) associated with thiazole group (in sulfathiazole), 4, 6-dimethylpyrimidin-2-yl group (in sulfamethazine), and 5-methyl-1, 2-oxazol-3-yl group (in sulfamethoxazole) at N position of sulfonamide group and lone pair electron reach N-atom (amino group in arene ring and in heterocyclic ring). Thus, Lewis acid base electronic interaction can also contribute to the total sorption affinities of the sulfonamides due to extra interaction of sulfonamide molecules with the lone pair electrons and protons of –COOH and –OH functional groups on the biochar surface [24]. The interaction can be written as:



where  $R_n = R_1/R_2/R_3$ .

Thus the adsorption of sulfonamides (both positive and negative species) would be possible with the mechanism of Lewis acid-base interaction as noted in reaction (7). It is expected that the lone pair electrons in the amino group and in hetero-N participate in the resonance process with the arene unit of sulfonamides, turning it into: firstly a positive species at low pH; and secondly, a negative species at higher pH. In these cases, Lewis acid-base interaction of sulfonamide antibiotics on the biochar surface may not be effective (**Figure 5**). However, this interaction might be possible at a pH where sulfonamides remain as a neutral species and thus, lone-pair electrons of amino groups in the arene unit may donate to form a complex with the protonated enriched surface functional groups. A few experiments with the addition of co-solutes (electron-acceptor groups such as 0.01 M  $\text{AlCl}_3$  and 0.025 M acetone in  $10 \text{ mg L}^{-1}$  SMT solution without adsorbent for 40 h) were conducted. It was observed that the pH change ( $\Delta\text{pH}$ ) was found to be 0.25-0.30 in neutral species regions. This

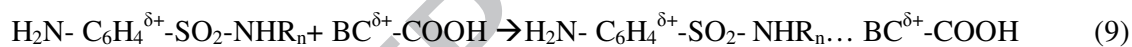
implied that the lone-pair-electrons availability from amino group or hetero-ring system of sulfonamides to electrons-acceptor groups were not significant and may be a small contributor to the reaction mechanism governed by the Lewis acid-base interactions. Experiments using only adsorbent and co-solutes resulted in significant pH change. This could be due to the release of protons into the solutions (**Table A7 and Figure A6**). Similar effects were also observed for the competition of co-solutes, the adsorbent and adsorbate; changes in final pH were due to the release of protons.

### 3.6. EDA and EAA ( $\pi$ - $\pi$ ) interactions

EDA interaction can be considered one of the main mechanisms for the sorption of positive species of sulfonamides on biochar surface [16, 34]. Stronger EDA interaction might be possible when the  $\pi$ -electron depletes aromatic ring (s) (or regions) and  $\pi$ -electron a rich regions (or aromatic rings) interact together [34]. More specifically, there is stronger interaction between oppositely polarized quadruples of functionalized sorbent surfaces and sorbate molecules in a parallel planar fashion. Sulfonamide molecules have a strong  $\pi$ -electron acceptor nature due to its amino functional groups (donates lone pair electrons to the benzene ring) and N and/or O-hetero-aromatic rings (contribution to electronic resonance). In contrast, the functionalized biochar surface was enriched with C=C, -OH, and -COOH functional groups based on our study using FTIR and Raman spectra (**Figures 6 and 7**) and other literatures [26, 35]. Hence, the surface functional groups of functionalized biochar can act as a strong  $\pi$ -electron-donor due its: firstly, hydroxyl groups being situated in the benzene rings (especially participating in resonance as a  $\pi$ -electron donor); and secondly, a strong  $\pi$ -electron-acceptor due to its carboxyl functional groups on the benzene rings (especially, protonated carboxyl groups that taking part in electronic resonance as a  $\pi$ -electron acceptor). In addition, the surface of functional biochar at low pH likely contains few, if any, negatively charged sites because we found the zeta-potential is positive below pH 2.5. The  $pK_a$  values

for carboxyl groups on aromatic ring systems are generally above 4.0 [16]. Subsequently, the surface of biochar may become positive due to protonation of unsaturated C atoms or heterocyclic N and/or S atoms.

When  $\pi$ -electron-acceptor is positively charged and this charge lies within or resonates with an arene unit of sulfonamides (e.g. charge in aromatic or heterocyclic aromatic amine) then a stabilized overall interaction is designed as  $\pi^+$ - $\pi$  EDA [16, 36]. Resonance forms of positive species of sulfonamides are able to form  $\pi^+$ -electron (acceptor site) and sorption affinities mostly governed by the mechanism of  $\pi^+$ - $\pi$  EDA. Teixidó et al. [16] presented clear support for  $\pi^+$ - $\pi$  EDA interactions of  $\text{SMT}^+$  in their study of solution pH and the effect of different cosolutes on cation exchange. Our study agrees with the literature in that the biochar surface contains -OH functional groups (equation 8). Moreover, donor-donor and acceptor-acceptor  $\pi$ -electron interaction might also be possible but not as strong as  $\pi$ - $\pi$  EDA interaction (equation 9) [37].



where  $\text{R}_n$  are aromatic heterogeneous groups in SMT, SMX and STZ.

It can also be hypothesized that the  $\pi$ - $\pi$  EAA mechanism between the positive species of sulfonamides arene units and surface carboxyl groups, which may also partially contribute the overall sorption but may not stabilize by charge repulsion. However, this also is not possible at very low pH due to  $\text{pK}_a$  values of surface carboxylic groups (more than 4) [38, 39]. The results on the effect of pH change showed very small change of pH both for single and competitive solutes (**Table A7**). Furthermore the release of proton in the solution from carboxylic groups might not occur which indicates that unfavorable to behave biochar surface to act as an electron acceptor at very low pH. Thus, the  $\pi$ - $\pi$  EAA interaction (reaction 3) can be ruled out for positive species of sulfonamides (**Figure 5**).

However, the maximum sorption capacities and  $K_d$  were found for the adsorption of sulfonamides neutral molecules only.



The reaction (equation 10) is unfavourable to exchange protons with water molecules by leaving the -OH group in the solution [31], thus solution pH should increase. We found, however, that pH shifted more to the acidic region after adsorption and this is backed up by the literature [16]. The proton transfer free energy  $\Delta G_{H^+}^0_{exch1} = -RT \ln(K_{a1}/K_{aw})$ , where  $K_{aw}$  is the water dissociation constant for sulfonamides with values ranging from +66.14 to +70.73  $\text{kJ mol}^{-1}$  (**Table 1**) [16]. The reaction in equation 11 shows the proton transfer from biochar surface functional groups (mostly -COOH rather than -OH) to amino N in sulfonamides molecules (-NH<sup>+</sup>.....O/OOC-BC). Furthermore proton transfer is likely not favourable by at least 15  $\text{kJ mol}^{-1}$  at 293 k at pH 5 [16], it is augmented by the strong H-bond that forms. The reaction in equation 12 involves tautomerisation of sulfonamides to the zwitterion in the adsorbed state while the reaction in equation 13 shows the tautomerisation by forming the zwitterion and releasing protons in the solution. Thus the observed pH decreased from the initial solution pH. The stabilization of reactions (equations 12 and 13) might be possible through the formation of a  $\pi^+-\pi$  EDA bond, which is not as strong as the positive species, of the positively charged sulfonamide ring system with the biochar surface. Overall stabilization of the cationic form of sulfonamides can be gained by releasing of a proton from surface functional groups so that a negative site can be provided. The aim here is for it to interact electrostatically with the positive charge through a strong H-bond formation. The  $\pi-\pi$  EAA interaction is less effective as biochar surface became negative above pH 2.5 and as surface carboxylate group has  $pK_a$  values of more than 4.

### 3.7. Hydrogen bonds formation and changing of pH

All peak assignments from the FTIR spectra and Raman spectra indicated that functionalized biochar contains  $\text{-OH}$ ,  $\text{-COOH}$  and  $\text{C=C}$  groups on the surface. In Raman spectra, two characteristic bands D-and-G can be assigned to carbon  $\text{SP}^2$  hybridization (**Table A8**) [26]. The D band relates to disordered  $\text{SP}^2$  hybridization of carbon atom containing vacancies, impurities or defects such as containing of oxygen containing functional groups. On the other hand, G band refers to the structural integrity of  $\text{SP}^2$  hybridization of carbon atoms. The intensity ratio of the D and G bands ( $I_D/I_G$ ) indicates the degree of graphitization. If the ratio is  $< 1$  then high degree of graphitization; if the ratio  $> 1$  then high number of functional groups present on the surface. The  $I_D/I_G$  ratio for biochar was 0.850, which was increased to 1.06 for functionalized biochar, indicating significantly increase in the number of functional groups on the functionalized biochar surface. Similar functional groups have been found in FTIR spectroscopy [15].

At higher pH where sulfonamide negative species dominate in the solution and the biochar surface becomes negative (zeta potential =  $-45.9$  mV), the anion exchange should be destabilized by charge repulsion. The adsorption of  $\text{SMT}^-$  was explained clearly by Teixidó et al. [16] who also noted that the adsorption was due solely or partially to adsorption of negative molecules by the release of  $\text{-OH}$  to proton exchange with water ( $\text{SMT}^- + \text{H}_2\text{O} \rightarrow \text{SMT}^0 + \text{OH}^-$ ), followed by interaction of the resulting natural molecules with surface  $\text{-COOH}$  and  $\text{-OH}$  functional groups ( $\text{SMT}^0 + \text{BC} = \text{SMT}^0 \dots \text{BC}$ ). This is supported by a strongly negative CAHB. As a result pH increased as the SMT sorption increased. On the other hand, we found that the final pH reduced to several units for all single and competitive sorption of sulfonamides antibiotics. The reduction of pH in the bank solutions were significant compared to single and competitive solution of antibiotics (**Table A7 and Figure A6**). Moreover, EDS analysis (average values) showed that the biochar particle comprised of carbon (81.17%) and oxygen (18.83%) with O/C atomic ratio of 0.23. Due to the

functionalization of biochar with  $oH_3PO_4$ , the O/C ratio increased significantly to 0.76 (51.96% C, 39.52% O and 8.16% P) (Table A.2). This indicates the functionalized biochar had a more oxidized surface [40]. Although  $H_xPO_4$  may be present in the core structure of functionalized biochar during preparation and surface  $H_xPO_4$  may undergo ligand exchange reactions with hydroxide and carboxyl groups, if any, in the solution (equation 14 and Figure 5) [41]. One might assume that significant of pH may be due to the capacity of biochar to release  $PO_4^{3-}$  ions [41]. However, our experiments observed no phosphate ion release during adsorption studies.



Thus the release of protons in the solution may be, solely, due to the presence of carboxyl groups on functionalized biochar. The carboxylate anion is stabilized by the resonance which delocalizes electronegativity between the two oxygen atoms. As a result carboxylates are ionized over a pH range. When electron-withdrawing groups such as =O or -Cl, are part of the same molecule, the  $pK_a$  value tends to decrease, whereas the presence of electron-donating alkyl groups tends to increase the  $pK_a$  [41]. The standard free energy of proton exchange is given by  $\Delta G_{H^+}^{0, \text{exch}2} = -RT \ln(K_{a2}/K_{aw})$  and  $pK_{a2}$  values of all sulfonamides ranged from 6.16 to 6.99. Furthermore the  $pK_a$  values of surface carboxyl groups are above 4 and those surface phenolic groups' values 10 or below [38]. Thus,  $\Delta pK_a$  value between surface carboxyl group and sulfonamide group is around 2.2-3 (for the surface hydroxyl group  $\approx 5$ ). As this difference narrows the bond between them becomes stronger. In the case of hydrogen dicarboxylate conjugate pairs  $[RCO_2 \dots H \dots O_2CR]^-$ , where  $\Delta pK_a$  is nearly zero and form a strong (-) CAHB [39]. The free energy of formation  $\Delta G_{(-)CAHB}^0$  in water can be estimated from gas-phase reaction and the resulting  $\Delta G_{(-)CAHB}^0$  is: firstly, about  $-56.2 \text{ kJ mol}^{-1}$  for the hydrogen dicarboxylic conjugate pair; and secondly, approximately  $-50.2 \text{ kJ mol}^{-1}$  for the hydrogen carboxylate-phenolate pair [39]. The free energy of proton release was calculated the from  $-SO_2\text{-NH-}$  as ranging from  $+38.38$  to  $+46.43 \text{ kJ mol}^{-1}$ , which is

unfavorable for proton release in the solution (**Table 1**). Thus,  $-\text{SO}_2\text{-NH-}$  can initially undergo for proton exchange with water molecule and release of  $-\text{OH}$  in solution (equation 9). The additional driving force may derive initially by the neutralization of  $-\text{OH}$  ions through the formation of negative CAHB (equation 10). Moreover, biochar surface  $-\text{COOH}$  group releases more protons into the solution leading to the reduction of final solution pH toward the neutral species region. Thus, a secondary increase in the sorption was found while studying the effect of pH. Thus change in pH toward neutral region provided the same mechanisms as described in neutral species sorption. In addition, according to reaction (equation 9),  $\pi\text{-}\pi$  EAA interaction now may be partially effective as biochar surface was highly negative and sulfonamide molecules also behave as negative species. When the solution pH maintained above 9, significantly reduction of pH was observed when electron-acceptor acetone cosolutes were present (**Table A7**).



Moreover, based on Raman and FTIR spectra for sorption of sulfonamides, it can be also confirm about hydrogen bond formation mechanisms. After sorption the FTIR peaks shifted to near positions, other points remained almost same, which indicated that adsorption did enhance at those particular wave-numbers. In addition, Raman  $I_D/I_G$  values decreased after sorption of both single and competitive solutes and this further indicated that a few bonds might form with the biochar surface and the sulfonamide molecules. Finally, the  $I_D/I_G$  ratio was found to be close to 1 suggesting that surface functional groups interacted with antibiotic molecules through may be strong H-bond formation (**Figure 7**). These bonds formation may be due to the protons linkage between biochar surface  $-\text{COOH}$  groups and antibiotics molecules.

#### 4. Conclusions

The details mechanisms of sulfonamide antibiotics sorption in both single and mixture mode were studied. The maximum sorption capacity of sulfonamides decreased as  $STZ > SMX > SMT$ . The sorption of sulfonamides occurred through the formation of  $\pi^+-\pi$  EDA for positive species, and through proton exchange with water molecules forming (-) CAHB and by  $\pi-\pi$  EAA interaction for negative species. The maximum sorption of sulfonamides was found for neutral species due to charge pairing through strong H-bond formation and stabilization of the zwitterion via  $\pi^+-\pi$  EDA mechanism. The results suggest that interactions between functionalized biochar and sulfonamide antibiotics can play important roles in the removal of emerging contaminants from water. Thus, it is believed that competitive sorption of a mixture of micropollutants onto functionalized biochar surface is environmentally significant and should be further extended to wastewater application.

### **Acknowledgements**

This research was funded by a Blue Sky Seed Fund from the Faculty of Engineering and Information Technology, University of Technology Sydney (2232137). Special thanks to Dr R. Shrestha for providing bamboo biomass samples.

### **Appendix A. Supplementary data**

### **References**

- [1] M. Seifrtová, L. Nováková, C. Lino, A. Pena, P. Solich, An overview of analytical methodologies for the determination of antibiotics in environmental waters, *Anal. Chim. Acta* 649 (2009) 158-179.
- [2] X. Guo, C. Yang, Z. Dang, Q. Zhang, Y. Li, Q. Meng, Sorption thermodynamics and kinetics properties of tylosin and sulfamethazine on goethite, *Chem. Eng. J.* 223 (2013) 59-67.

- [3] M.B. Ahmed, J.L. Zhou, H.H. Ngo, W. Guo, Adsorptive removal of antibiotics from water and wastewater: Progress and challenges, *Sci. Total Environ.* 532 (2015) 112-126.
- [4] A.B. Boxall, D.W. Kolpin, B. Halling-Sørensen, J. Tolls, Peer reviewed: are veterinary medicines causing environmental risks?, *Environ. Sci. Technol.* 37 (2003) 286A-294A.
- [5] Y. Li, X. Wu, Z. Li, S. Zhong, W. Wang, A. Wang, J. Chen, Fabrication of CoFe<sub>2</sub>O<sub>4</sub>-graphene nanocomposite and its application in the magnetic solid phase extraction of sulfonamides from milk samples, *Talanta* 144 (2015) 1279-1286.
- [6] M.B. Ahmed, J.L. Zhou, H.H. Ngo, W. Guo, N.S. Thomaidis, J. Xu, Progress in the biological and chemical treatment technologies for emerging contaminant removal from wastewater: a critical review, *J. Hazard. Mater.* 323 (2017) 274-298.
- [7] G.T. Ankley, B.W. Brooks, D.B. Huggett, J. P. Sumpter, Repeating history: pharmaceuticals in the environment, *Environ. Sci. Technol.* 41 (2007) 8211-8217.
- [8] A.E. Creamer, B. Gao, S. Wang, Carbon dioxide capture using various metal oxyhydroxide-biochar composites, *Chem. Eng. J.* 283 (2016) 826-832.
- [9] M. Jia, F. Wang, X. Jin, Y. Song, Y. Bian, L.A. Boughner, L. A., X. Yang, C. Gu, X. Jiang, Q. Zhao, Metal ion-oxytetracycline interactions on maize straw biochar pyrolyzed at different temperatures. *Chem. Eng. J.* 304 (2016), 934-940.
- [10] X.R. Jing, Y.Y. Wang, W.J. Liu, Y.K. Wang, H. Jiang, Enhanced adsorption performance of tetracycline in aqueous solutions by methanol-modified biochar, *Chem. Eng. J.* 248 (2014) 168-174.
- [11] Y. Yao, B. Gao, H. Chen, L. Jiang, M. Inyang, A.R. Zimmerman, X. Cao, L. Yang, Y. Xue, H. Li, Adsorption of sulfamethoxazole on biochar and its impact on reclaimed water irrigation, *J. Hazard. Mater.* 209 (2012) 408-413.
- [12] K.K. Shimabuku, J.P. Kearns, J.E. Martinez, R.B. Mahoney, L. Moreno-Vasquez, R.S. Summers, Biochar sorbents for sulfamethoxazole removal from surface water, stormwater, and wastewater effluent, *Water Res.* 96 (2016) 236-245.

- [13] F. Lian, B. Sun, Z. Song, L. Zhu, X. Qi, B. Xing, Physicochemical properties of herb-residue biochar and its sorption to ionizable antibiotic sulfamethoxazole, *Chem. Eng. J.* 248 (2014) 128-134.
- [14] M.B. Ahmed, J.L. Zhou, H.H. Ngo, W. Guo, Insight into biochar properties and its cost analysis, *Biomass Bioenerg.* 84 (2016) 76-86.
- [15] M.B. Ahmed, J.L. Zhou, H.H. Ngo, W. Guo, M. Chen, Progress in the preparation and application of modified biochar for improved contaminant removal from water and wastewater, *Bioresour. Technol.* 214 (2016) 836-851.
- [16] M. Teixidó, J.J. Pignatello, J.L. Beltrán, M. Granados, J. Peccia, Speciation of the ionizable antibiotic sulfamethazine on black carbon (biochar), *Environ. Sci. Technol.* 45 (2011) 10020-10027.
- [17] H. Zheng, Z. Wang, J. Zhao, S. Herbert, B. Xing, Sorption of antibiotic sulfamethoxazole varies with biochars produced at different temperatures, *Environ. Pollut.* 181 (2013) 60-67.
- [18] L. Ji, W. Chen, S. Zheng, Z. Xu, D. Zhu, Adsorption of sulfonamide antibiotics to multiwalled carbon nanotubes, *Langmuir* 25 (2009) 11608-11613.
- [19] L. Ji, Y. Wan, S. Zheng, D. Zhu, Adsorption of tetracycline and sulfamethoxazole on crop residue-derived ashes: implication for the relative importance of black carbon to soil sorption, *Environ. Sci. Technol.* 45 (2011) 5580-5586.
- [20] C. Gan, Y. Liu, X. Tan, S. Wang, G. Zeng, B. Zheng, T. Li, Z. Jiang, W. Liu, Effect of porous zinc-biochar nanocomposites on Cr (vi) adsorption from aqueous solution, *RSC Advances* 5 (2015) 35107-35115.
- [21] S. Teixeira, C. Delerue-Matos, L. Santos, Removal of sulfamethoxazole from solution by raw and chemically treated walnut shells, *Environ. Sci. Pollut. Res.* 19 (2012) 3096-3106.
- [22] S. Wan, Z., Hua, L. Sun, Z. Bai, L. Liang, Biosorption of nitroimidazole antibiotics onto chemically modified porous biochar prepared by experimental design: kinetics,

thermodynamics, and equilibrium analysis, *Process Saf. Environ. Protect.* 104 (2016) 422-435.

[23] M. Xie, W. Chen, Z. Xu, S. Zheng, D. Zhu, Adsorption of sulfonamides to demineralized pine wood biochars prepared under different thermochemical conditions, *Environ. Pollut.* 186 (2014) 187-194.

[24] H. Zhao, X. Liu, Z. Cao, Y. Zhan, X. Shi, Y. Yang, J. Zhou, J. Xu, Adsorption behavior and mechanism of chloramphenicols, sulfonamides, and non-antibiotic pharmaceuticals on multi-walled carbon nanotubes, *J. Hazard. Mater.* 310 (2016) 235-245.

[25] X.R. Jing, Y.Y. Wang, W.J. Liu, Y.K. Wang, H. Jiang, Enhanced adsorption performance of tetracycline in aqueous solutions by methanol-modified biochar, *Chem. Eng. J.* 248 (2014) 168-174.

[26] C. Zhang, C. Lai, G. Zeng, D. Huang, C. Yang, Y. Wang, Y. Zhou, M. Cheng, Efficacy of carbonaceous nanocomposites for sorbing ionizable antibiotic sulfamethazine from aqueous solution, *Water Res.* 95 (2016) 103-112.

[27] A.U. Rajapaksha, M. Vithanage, M. Ahmad, D.C. Seo, J.S. Cho, S.E. Lee, S.S. Lee, Y.S. Ok, Enhanced sulfamethazine removal by steam-activated invasive plant-derived biochar, *J. Hazard. Mater.* 290 (2015) 43-50.

[28] F. Wang, W. Sun, W. Pan, N. Xu, Adsorption of sulfamethoxazole and 17 $\beta$ -estradiol by carbon nanotubes/CoFe<sub>2</sub>O<sub>4</sub> composites, *Chem. Eng. J.* 274 (2015) 17-29.

[29] F.F. Liu, J. Zhao, S. Wang, B. Xing, Adsorption of sulfonamides on reduced graphene oxides as affected by pH and dissolved organic matter, *Environ. Pollut.* 210 (2016) 85-93.

[30] B. Sun, F. Lian, Q. Bao, Z. Liu, Z. Song, L. Zhu, Impact of low molecular weight organic acids (LMWOAs) on biochar micropores and sorption properties for sulfamethoxazole, *Environ. Pollut.* 214 (2016) 142-148.

- [31] M.K. Richter, M. Sander, M. Krauss, I. Christl, M.G. Dahinden, M.K. Schneider, R.P. Schwarzenbach, Cation binding of antimicrobial sulfathiazole to leonardite humic acid, *Environ. Sci. Technol.* 43 (2009) 6632-6638.
- [32] M. Kahle, C. Stamm, time and pH-dependent sorption of the veterinary antimicrobial sulfathiazole to clay minerals and ferrihydrite, *Chemosphere* 68 (2007) 1224-1231.
- [33] X. Zhang, W. Guo, H.H. Ngo, H. Wen, N. Li, W. Wu, Performance evaluation of powdered activated carbon for removing 28 types of antibiotics from water, *J. Environ. Manag.* 172 (2016) 193-200.
- [34] W. Chen, L. Duan, L. Wang, D. Zhu, Adsorption of hydroxyl-and amino-substituted aromatics to carbon nanotubes, *Environ. Sci. Technol.* 42 (2008) 6862-6868.
- [35] S. Zhang, Z. Min, H.L. Tay, M. Asadullah, C.Z. Li, Effects of volatile-char interactions on the evolution of char structure during the gasification of Victorian brown coal in steam, *Fuel* 90 (2011) 1529-1535.
- [36] H. Wijnja, J.J. Pignatello, K. Malekani, Formation of  $\pi$ - $\pi$  complexes between phenanthrene and model  $\pi$ -acceptor humic subunits, *J. Environ. Qual.* 33 (2004) 265-275.
- [37] D. Zhang, B. Pan, H. Zhang, P. Ning, B. Xing, Contribution of different sulfamethoxazole species to their overall adsorption on functionalized carbon nanotubes, *Environ. Sci. Technol.* 44 (2010) 3806-3811.
- [38] J. Ni, J.J. Pignatello, B. Xing, Adsorption of aromatic carboxylate ions to black carbon (biochar) is accompanied by proton exchange with water, *Environ. Sci. Technol.* 45 (2011) 9240-9248.
- [39] P. Gilli, L. Pretto, V. Bertolasi, G. Gilli, Predicting hydrogen-bond strengths from acid-base molecular properties. The  $pK_a$  slide rule: Toward the solution of a long-lasting problem, *Acc. Chem. Res.* 42 (2008) 33-44.
- [40] F. Yang, L. Zhao, B. Gao, X. Xu, X. Cao, The interfacial behavior between biochar and soil minerals and its effect on biochar stability, *Environ. Sci. Technol.* 50 (2016) 2264-2271.

[41] J. Lehmann, S. Joseph, Biochar for environmental management: science, technology and implementation, Routledge 2015.

ACCEPTED MANUSCRIPT

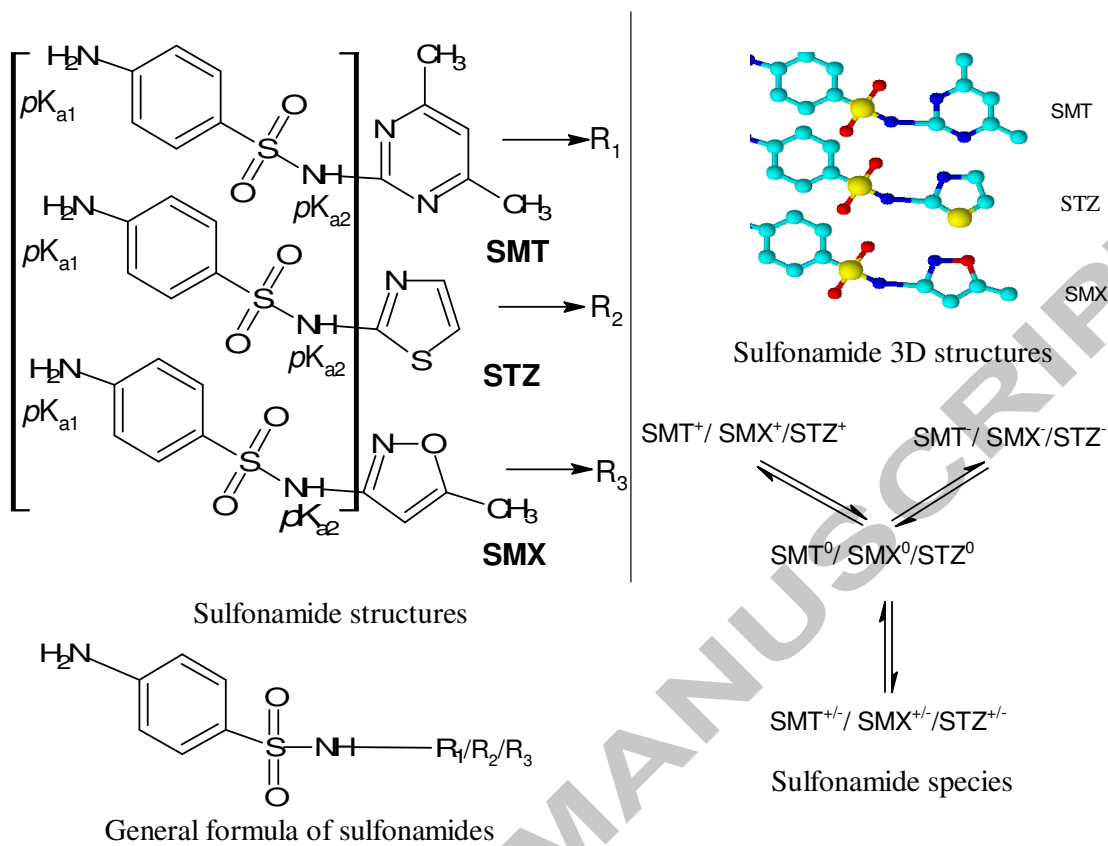


**Figure 1.** Molecular structures of sulfonamides antibiotics and their equilibrium species.

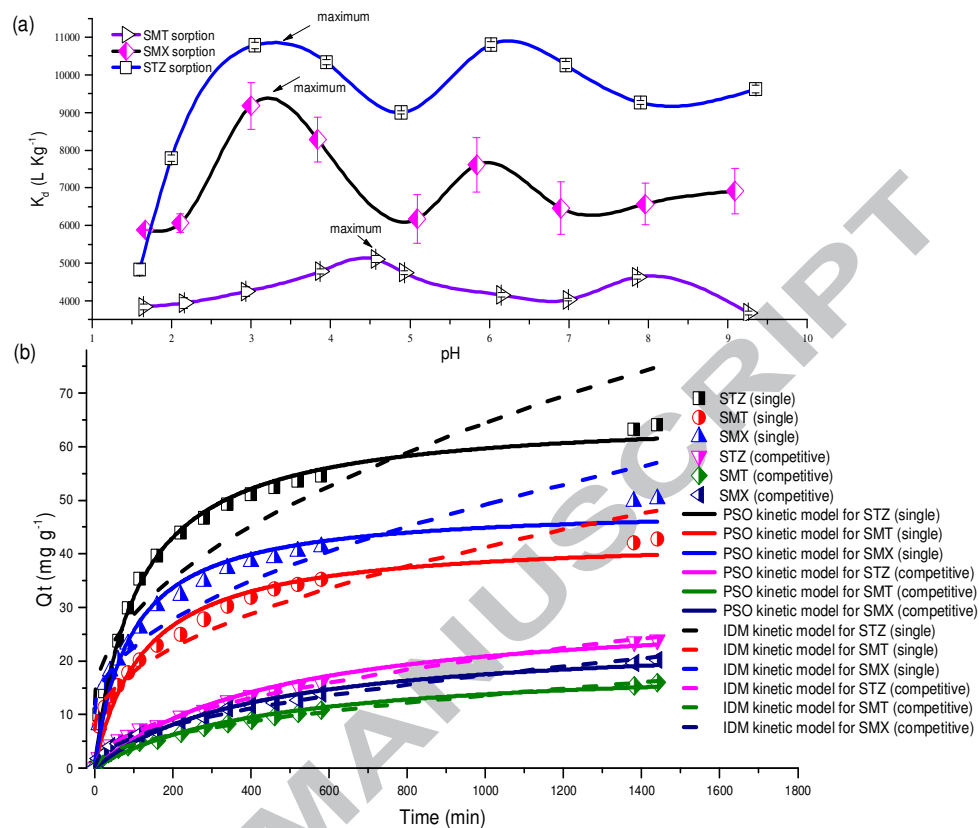


**Figure 2.** (a) Effect of pH on the distribution coefficient ( $K_d$ ) with standard deviation (error bars) for removal of sulfonamide antibiotics; (b) single and competitive sorption kinetics data with PSO and IDM kinetics model fittings (initial concentration of sulfonamide antibiotics being 10 mg L<sup>-1</sup> for single solute, and 3.33 mg L<sup>-1</sup> for each competitive solute at room temperature using 100 mg L<sup>-1</sup> functionalized biochar dosages).

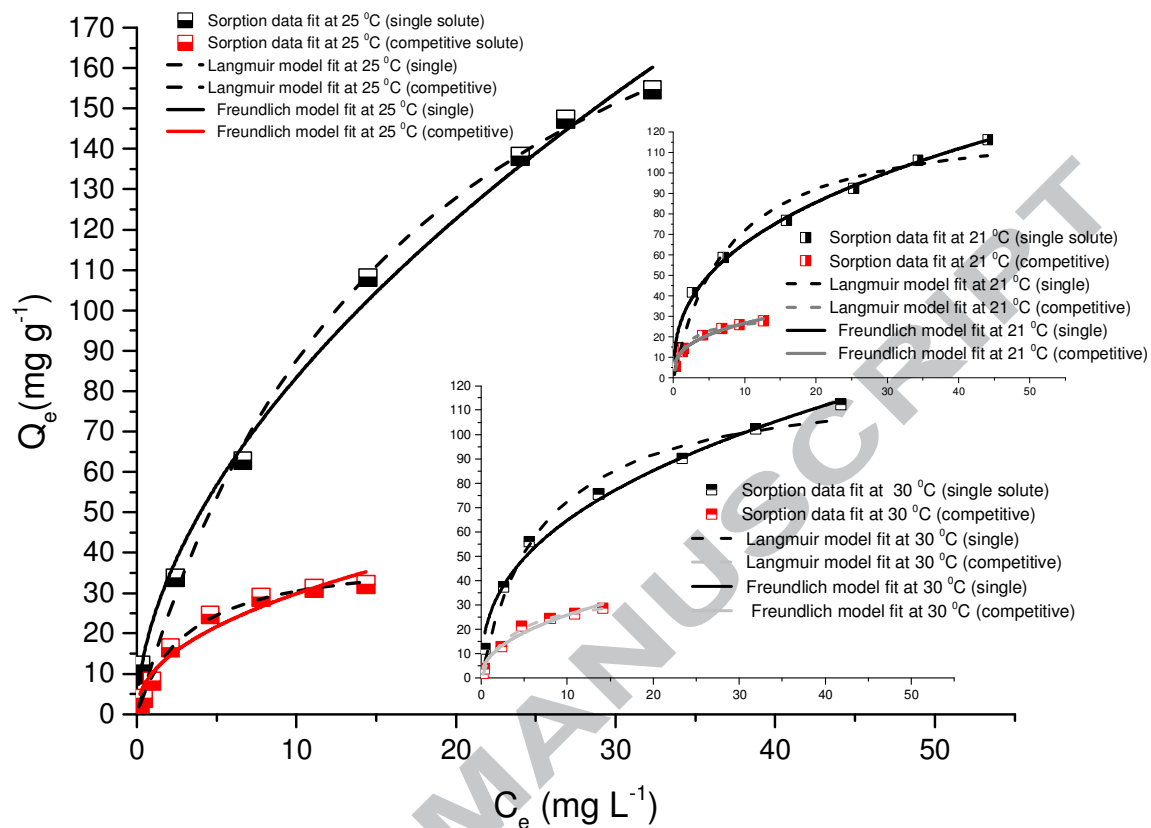


**Figure 3.** STZ adsorption isotherm plots and model fits from single solute (initial concentration 0.5-50 mg L<sup>-1</sup>), and from mixtures (initial individual concentrations were 0.33-16.67 mg L<sup>-1</sup>) at pH 3.5 and different temperatures.

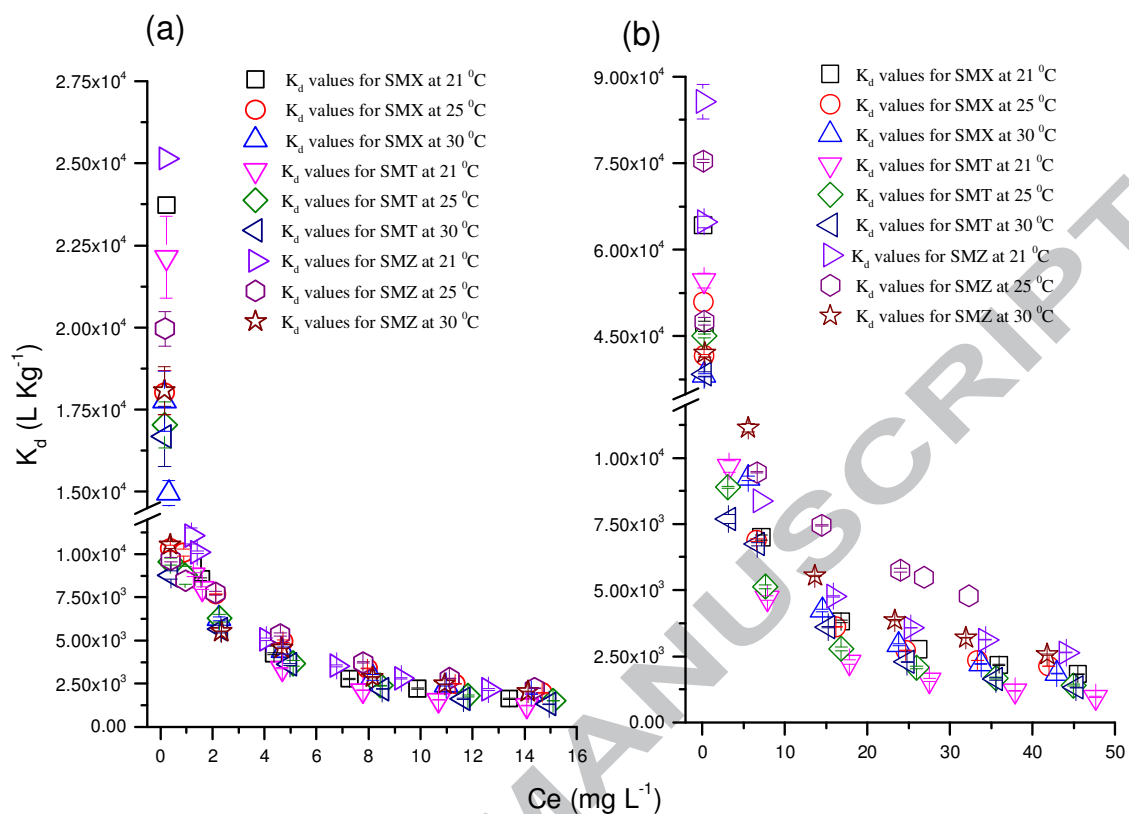


**Figure 4.** Change of  $K_d$  values (with SD as error bars) against equilibrium concentrations for (a) competitive solutes with total initial solution concentrations ( $C_0$ ) at 1-50  $mg\ L^{-1}$  and each solute concentration was 0.33-16.67  $mg\ L^{-1}$  (i.e.  $C_0/3$ ), and for (b) single solute ( $C_0 = 0.5$ -50  $mg\ L^{-1}$ ).

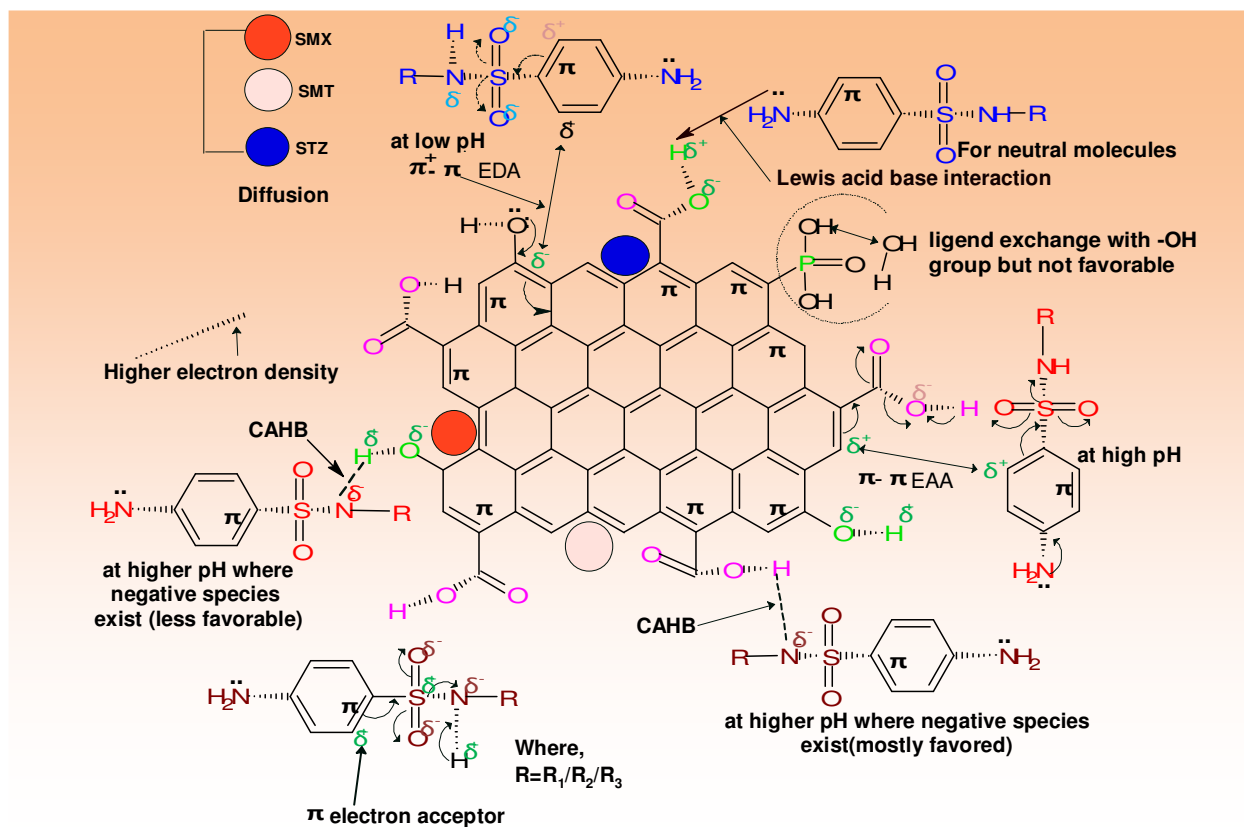


**Figure 5.** Proposed sorption mechanism for single and competitive antibiotics ( $R_1$  for SMT,  $R_2$  for STZ,  $R_3$  for SMX) on functionalized biochar with possible resonance effects for  $\pi$ - $\pi$  interactions.

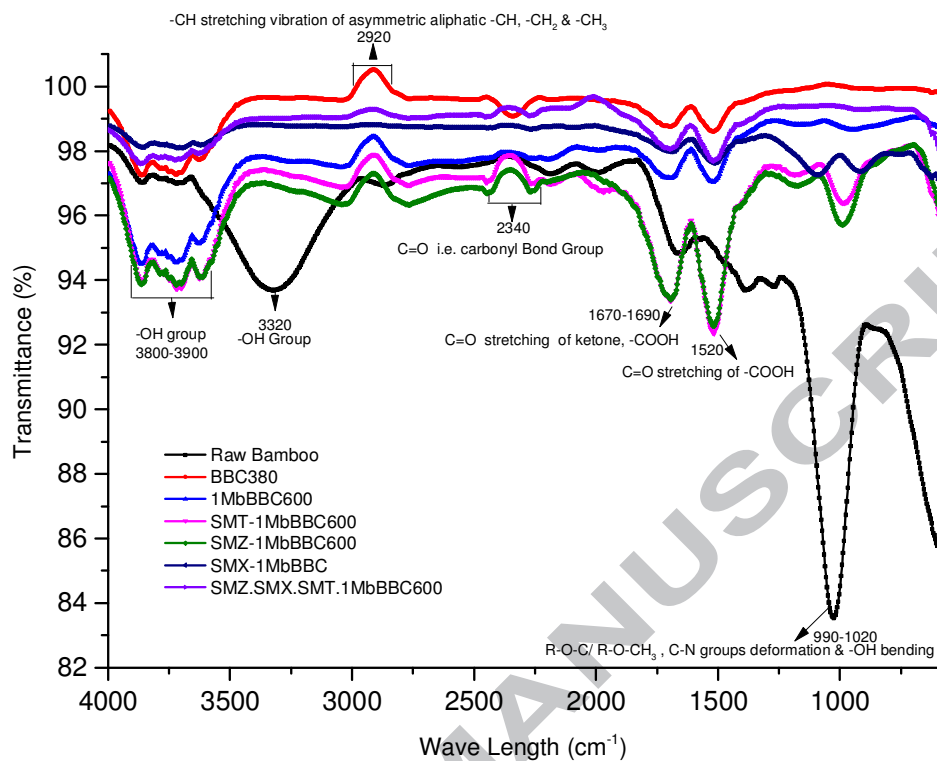


**Figure 6.** FTIR spectra for raw bamboo biomass, biochar (BBC380), and functionalized biochar (1MbBBC600) for the sorption of single and competitive solutes (before and after adsorption).

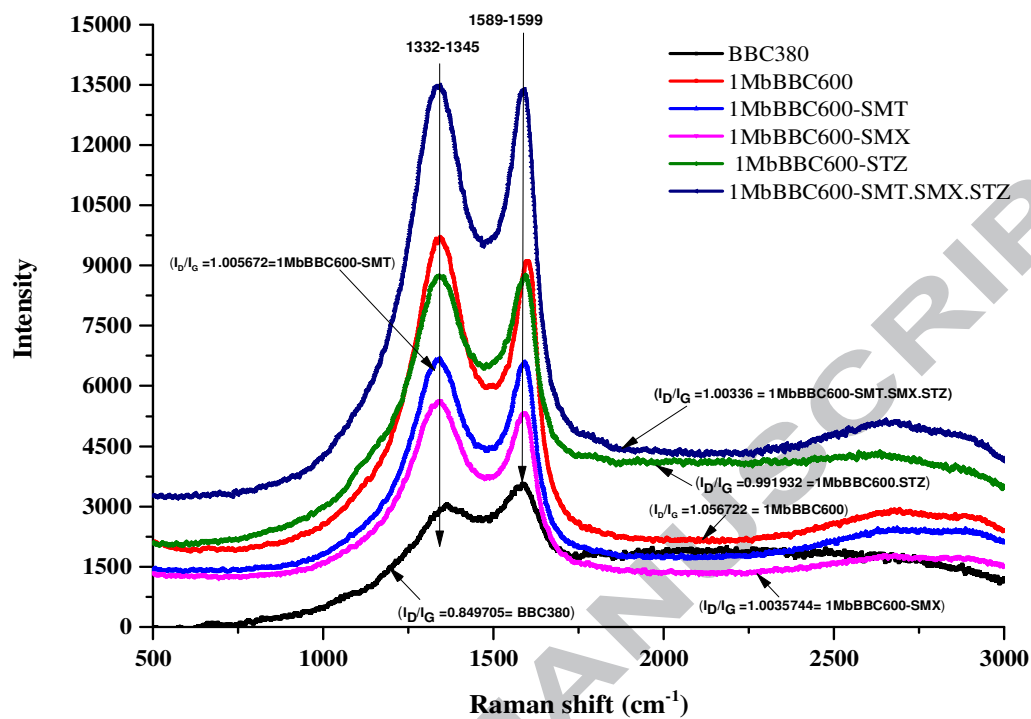
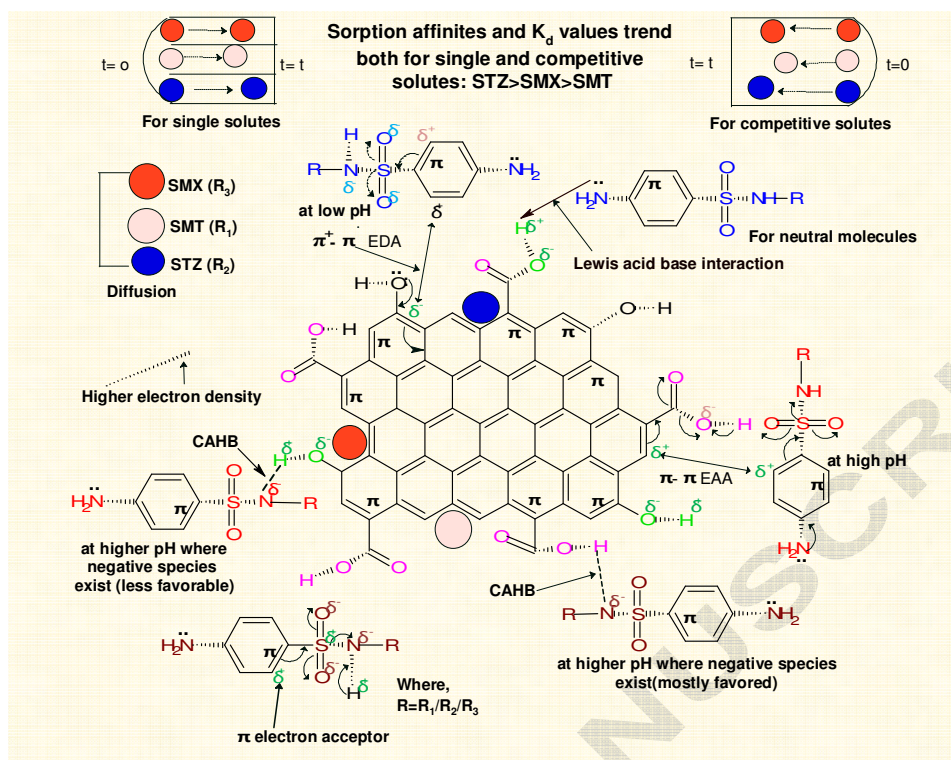


**Figure 7.** Raman spectra with band ratio ( $I_D/I_G$ ) for biochar (BBC380), and functionalized biochar (1MbBBC600) before and after sorption of single and competitive solutes.

**Table 1.**  $\Delta G^0$  values calculated from water dissociation constant ( $K_{aw}$ ) at different temperatures.

Compound	Temp (K)	pK <sub>a1</sub>	pK <sub>a2</sub>	K <sub>aw</sub>	RT Ln K <sub>aw</sub>	RT ln K <sub>aw</sub> (in kJ mol <sup>-1</sup> )	RT ln K <sub>a1</sub> (in kJ mol <sup>-1</sup> )	RT ln K <sub>a2</sub> (in kJ mol <sup>-1</sup> )	$\Delta G_{H^+}^{0, exch1}$ (in kJ mol <sup>-1</sup> )	$\Delta G_{H^+}^{0, exch2}$ (in kJ mol <sup>-1</sup> )
SMX	294	1.97	6.1	$6.85 \times 10^{-15}$	-	-79.72	-11.09	-34.67	68.63	45.05
			6		79720					
	298	1.97	6.1	$6.85 \times 10^{-15}$	-	-80.81	-11.24	-35.14	69.57	45.66
			6		80805					
	303	1.97	6.1	$6.85 \times 10^{-15}$	-	-82.16	-11.43	-35.73	70.73	46.43
			6		82161					
STZ	293	2.04	6.9	$1.01 \times 10^{-14}$	-	-78.51	-11.44	-38.87	67.07	39.64
			3		78508					
	298	2.04	6.9	$1.01 \times 10^{-14}$	-	-79.85	-11.64	-39.54	68.21	40.31
			3		79848					
	303	2.04	6.9	$1.01 \times 10^{-14}$	-	-81.2	-11.83	-40.20	69.36	40.99
			3		81188					
SMT	293	2.04	6.9	$1.47 \times 10^{-14}$	-	-77.59	-11.44	-39.21	66.14	38.38
			9		77587					
	298	2.04	6.9	$1.47 \times 10^{-14}$	-	-78.91	-11.64	-39.88	67.27	39.04
			9		78911					
	303	2.04	6.9	$1.47 \times 10^{-14}$	-	-80.24	-11.83	-40.55	68.40	39.69
			9		80235					

- K<sub>aw</sub> values were taken from <http://www.chemguide.co.uk/physical/acidbaseeqia/kw.html>
- pK<sub>a1</sub> and pK<sub>a2</sub> were taken from **Table A1** and  $R = 8.314 \text{ (J K}^{-1} \text{ mol}^{-1}\text{)}$  and  $\Delta G_{H^+}^{0, exch1/2} = -RT \ln(K_{a1/a2} / K_{aw})$



**Highlights**

- Functionalized biochar can sorb antibiotics in both single and competitive mode
- Sorption capacity for antibiotics was three times higher in single mode than in competitive mode
- Sorption capacity decreases as sulfathiazole > sulfamethoxazole > sulfamethazine
- Solution pH is a significant parameter for removing ionisable sulfonamides
- Sorption is mostly governed by the H-bonds formation and  $\pi$ - $\pi$  interactions

ACCEPTED MANUSCRIPT